Intriguingly, the time course of extinction varied in our study, depending on whether the agent was predator- or area-related. Spider populations on islands with predators never increased above initial (introduction) sizes. In contrast, among predator-free islands, spiders on small islands frequently showed rapid population growth initially, even sometimes outstripping growth on large islands (*22*). Nonetheless, all those populations eventually became extinct, in contrast to some on large islands which have now persisted for 12 years since the initial introduction. Given possible variation in both natural and human-induced immigration rates, such differences allow insight into the temporal dynamics of species preservation.

REFERENCES AND NOTES

1. J. Diamond and T. J. Case, in *Community Ecology*, J. Diamond and T. J. Case, Eds. (Harper and Row, New York, 1986), pp. 65–79; S. L. Pimm, *The Balance of Nature?* (Univ. of Chicago Press, Chicago, IL, 1991).
2. K. L. Crowell, *Am. Nat.* **107**, 535 (1973); M. V. Lomolino, *ibid.* **123**, 468 (1984); T. Ebenhard, *J. Biogeogr.* **14**, 213 (1987).
3. T. W. Schoener and A. Schoener, *Nature* **302**, 332 (1983).
4. T. W. Schoener and C. A. Toft, *Science* **219**, 1353 (1983).
5. C. A. Toft and T. W. Schoener, *Oikos* **41**, 411 (1983); T. W. Schoener, in *Community Ecology*, J. Diamond and T. J. Case, Eds. (Harper and Row, New York, 1986), pp. 556–586.
6. Birds and other predators of spiders may be more common on islands with lizards, but removals (*13*) and introductions (*23*) of lizards implicate the latter as causal.
7. T. W. Schoener and C. A. Toft, *Behav. Ecol. Sociobiol.* **12**, 121 (1983); D. A. Spiller and T. W. Schoener, *J. Anim. Ecol.* **58**, 509 (1989).
8. In the second introduction, individuals were released at three closely adjacent sites in groups of five, one of which sites was the same as in the first introduction.
9. To assay survival, we first identified each resident female on the five islands still having them by tagging her web and noting her body size. After 4 days, when censusing for survival of introduced spiders, we did not include individuals in or near tagged webs that were the same size as the appropriate residents.
10. Introductions and yearly censuses were done in May or very late April, 1982 through 1987. Census methods were as described (*4, 5*).
11. *P* values are from contrasts (df = 1, 12) in repeated-measures analysis of variance (ANOVA), one-tailed tests. Frequencies were arcsine–square root transformed before analysis. Sequential Bonferroni tests (*16*) at $\alpha = 0.05$ were used to adjust for multiple comparisons; all *P* values given in the paper are raw (that is, uncorrected for multiple comparisons). Because propagule size and certain other conditions (*12*) were different for the two phases, separate analyses of survival were also done (contrast $P = 0.003$, 0.215 for the first and second hypothesis, respectively, for Phase 1; $P = 0.016$, >0.5, respectively, for Phase 2); the first hypothesis in each phase is significant with a sequential Bonferroni test. Nonetheless, in repeated measures, neither the phase ($P = 0.507$) nor phase-treatment ($P = 0.548$) source of variation was significant, causing rejection of hypotheses of survival differences associated with the two phases. All analyses in this paper were done with SAS software.
12. Although other explanations are possible, weak evidence exists that spiders apparently remaining from the first introduction had a positive effect: Islands with a large number (20 to 35) of already-established spiders had greater survivorship than did the other islands without lizards (mean survival frequencies 0.93 versus 0.70; equal variances $t = 1.92$, two-tailed test, $P = 0.091$).
13. T. W. Schoener and D. A. Spiller, *Science* **236**, 949 (1987); D. A. Spiller and T. W. Schoener, *Ecol. Monogr.* **58**, 57 (1988); *Oecologia* **83**, 150 (1990); *Ecology* **75**, 182 (1994).
14. A. L. Turnbull, *Annu. Rev. Entomol.* **18**, 305 (1973).
15. All population sizes were log(x + 1)-transformed before analysis. Contrasts used one-tailed tests.
16. W. R. Rice, *Evolution* **43**, 223 (1989).
17. Mauchly's Sphericity Test is not significant ($P = 0.137$), allowing acceptance of sphericity, so we report unadjusted *P* values [as recommended in R. J. Freund, R. C. Littell, P. C. Spector, *SAS system for Linear Models* (SAS Institute, Cary, NC, 1986); our design, in which time is the repeated factor, follows the example in this source (see chapter 6)]. The Huynh-Feldt (H-F) Epsilon is very high (0.961), and the H-F adjusted probabilities are very close to those we report. Multivariate repeated-measures evaluations ('Wilks') are not significant [in the order given in text, $P = 0.230$ (df = 4, 9), $P = 0.376$ (df = 8, 18), $P = 0.158$ (df = 4, 9) and $P = 0.600$ (df = 4, 9)], but for our design the multivariate procedure has statistical power below that recommended, and assuming sphericity allows one to use the univariate results [J. Stevens, *Applied Multivariate Statistics for the Social Sciences* (Erlbaum, Hillsdale, NJ, ed. 2, 1992)]. Unequal variances of the treatments implies that these ANOVAs should be interpreted cautiously. With the use of the means of the five census times, separate *F*-tests lead to the conclusion that variances of the two large-island types are unequal, whereas those of the two no-lizard types are not. The appropriate separate *t* tests give $P = 0.025$ and $P = 0.071$, respectively, for the two contrasts.
18. However, the interaction between time and the contrast of large versus small islands without lizards has raw $P = 0.063$. Univariate and multivariate repeated-measures analyses are identical here.
19. T. W. Schoener, *Oikos* **41**, 372 (1983); T. W. Schoener and D. A. Spiller, *Nature* **330**, 474 (1987).
20. T. E. Lovejoy and D. C. Oren, in *Forest Dynamics in Man-Dominated Landscapes*, R. L. Burgess and D. M. Sharp, Eds. (Springer-Verlag, New York, 1981), pp. 8–12; G. R. Robinson and J. F. Quinn, in *Applied Population Biology*, S. K. Jain and L. W. Botsford, Eds. (Kluwer Academic, Norwell, MA, 1992), pp. 223–248.
21. However, a moderate number of nonexperimental studies of the effect of predators on invasion success exist [for example, R. D. Goeden and S. M. Louda, *Annu. Rev. Entomol.* **21**, 325 (1976); D. Simberloff, in *Ecology of Biological Invasions of North America and Hawaii*, H. A. Mooney and J. A. Drake, Eds. (Springer-Verlag, New York, 1986)]. The first reference underscores the paucity of experimental studies and calls for the sort of investigation done here.
22. This could be positive density dependence, given the smaller potential area for mate location on smaller islands. Possible factors causing small-island populations eventually to become extinct include severe storms, drought, depletion by spiders of their own prey organisms, and emigration, as well as demographic stochasticity characterizing small populations.
23. T. W. Schoener and D. A. Spiller, in preparation.

24. We thank E. Temeles and C. Toft for field assistance and NSF for support.

31 August 1994; accepted 12 January 1995

Demonstration of Positionally Disordered Water Within a Protein Hydrophobic Cavity by NMR

James A. Ernst, Robert T. Clubb, Huan-Xiang Zhou, Angela M. Gronenborn,* G. Marius Clore*

The presence and location of water of hydration (that is, bound water) in the solution structure of human interleukin-1β (hIL-1β) was investigated with water-selective two-dimensional heteronuclear magnetic resonance spectroscopy. It is shown here that in addition to water at the surface of the protein and ordered internal water molecules involved in bridging hydrogen bonds, positionally disordered water is present within a large, naturally occurring hydrophobic cavity located at the center of the molecule. These water molecules of hydration have residency times in the range of 1 to 2 nanoseconds to 100 to 200 microseconds and can be readily detected by nuclear magnetic resonance (NMR). Thus, large hydrophobic cavities in proteins may not be truly empty, as analysis of crystal structures appears to show, but may contain mobile water molecules that are crystallographically invisible but detectable by NMR.

Water of hydration (that is, bound water) has long been known to play an important structural and functional role in proteins (*1*). In particular, buried water molecules may stabilize protein structure by acting as bridges between protein hydrogen bond donors and acceptors, whereas surface water molecules located at the active site participate in catalysis and ligand recognition. Experimentally, bound water can be detected either in the crystal state by x-ray and neutron diffraction or in solution by NMR spectroscopy. Only positionally ordered water molecules can be detected in crystal structures, as the observed electron density represents a linear superposition of all the atomic positions during the course of the experiment (which typically lasts many hours). Thus, the detection of a water molecule at a given location in the crystal structure, although independent of its residency time, requires that the potential of mean force at this point has a well-defined

Laboratory of Chemical Physics, National Institute of Diabetes and Digestive and Kidney Diseases, National Institutes of Health, Bethesda, MD 20892, USA.

*To whom correspondence should be addressed.

local minimum such that a water molecule always returns to the same position, thereby giving rise to observable electron density (*2*). If this is not the case, the resulting electron density will be smeared and, as a result, undetectable. In this light, it is not surprising that water molecules observed in crystal structures are almost invariably hydrogen-bonded either directly or indirectly by means of a hydrogen-bonded water network to polar backbone or side chain groups of the protein (*1*, *3*). The detection of water molecules by NMR, on the other hand, does not require uniform ordering but is dependent only on the spatial proximity of water protons to protons of the protein and the lifetime of the bound water (*4*, *5*).

Although the interiors of proteins are generally well packed (*6*), the packing is not always perfect, which results in the presence of cavities (*7*). In addition, cavities have been generated artificially by replacement of larger side chains with smaller ones (*8*, *9*). Although water molecules have been observed crystallographically in polar cavities, there is only one example of ordered water molecules in a small hydrophobic cavity (*10*). Indeed, all the hydrophobic cavities generated in T4 lysozyme ranging in volume from 34 to 215 $Å^3$ appear to be empty in the corresponding crystal structures (*8*). Likewise, analysis of the crystal structures of a series of cavity-generating mutants in ribonuclease A showed that cavities with an apolar character are empty (*9*). These observations seem to be supported by recent measurements of solubility and vapor pressure, which suggest that it is unlikely that single water molecules enter small, nonpolar cavities in proteins (*11*). Here, we present an NMR analysis of bound water in human interleukin-1β (hIL-1β), a β sheet protein with a β-trefoil fold (*12*) whose structure has been solved by both crystallography (*13*) and NMR (*14*).

Through-space interactions between aliphatic protons of ^{13}C-labeled hIL-1β and bound water were detected with the use of two-dimensional (2D) ^{12}C-filtered H_2O–nuclear Overhauser enhancement (NOE)–^1H-^{13}C and H_2O–rotating frame Overhauser enhancement (ROE)–^1H-^{13}C heteronuclear single quantum coherence (HSQC) spectra recorded at several mixing times and temperatures (*15*). These experiments use low-power ^1H pulses (70 to 100 Hz) to selectively invert the water resonance and are very sensitive because the slowly relaxing water is never saturated (*16*, *17*). Each experiment consists of two interleaved data sets in which the ^1H water magnetization lies either parallel ($+z$) or antiparallel ($-z$) to the magnetization of the protein ^1H resonances, which are aligned along the $+z$ direction before the NOE and ROE mixing times. The difference between the two data sets provides a protein-water NOE or ROE difference spectrum that contains cross-peaks arising solely from interactions between protein and water protons (*16*, *17*). An example of two regions of the 60-ms mixing time of the H_2O-NOE-^1H-^{13}C HSQC difference spectrum recorded at 35°C is shown in Fig. 1.

Cross-peaks in these spectra may arise from either a direct through-space interaction between ^{13}C-attached protein protons and water protons separated by ≤5 Å or by an indirect pathway involving an NOE or ROE between ^{13}C-attached protons and exchangeable protons of the protein (such as a hydroxyl group of Ser, Thr, and Tyr, the ε-NH_3 group of Lys, or the guanidino group of Arg) followed by chemical exchange with water (*4*, *5*). Over 200 cross-peaks could be detected, 95 of which could be attributed to a direct NOE or ROE interaction with bound water because the relevant protein protons were more than 5 Å from any exchangeable groups. The locations of these protons abstracted to the directly bonded carbon atoms and superimposed on the backbone of hIL-1β are shown in Fig. 2. All the observed NOEs are negative in sign, indicating that the residence times of the bound water molecules have to be greater than ~500 ps. Moreover, once the residence time exceeds the rotational correlation time (in this case, ~8 ns) by a factor of ≥3, the NOE intensities will be independent of residence time.

Analysis of the three independently solved x-ray structures of hIL-1β (*13*) reveals the presence of 26 conserved water molecules, defined as water molecules common to all three structures whose oxygen atoms have an average atomic root mean square displacement of 1 Å or less. Of these, 19 were potentially identifiable by NMR (that is, they are less than 5 Å away from nonexchangeable protein protons that themselves are further than 5 Å away from potentially exchangeable protons), and 10 were actually observed (magenta in Fig. 2). These 10 water molecules are all involved in bridging backbone hydrogen bonds, and 7 of them were previously detected in 3D ^{15}N-edited ROE spectra (*5*, *14*).

Most interactions with bound water in our experiments involved methyl groups. This is a result of their favorable spectral properties, namely narrow lines and high

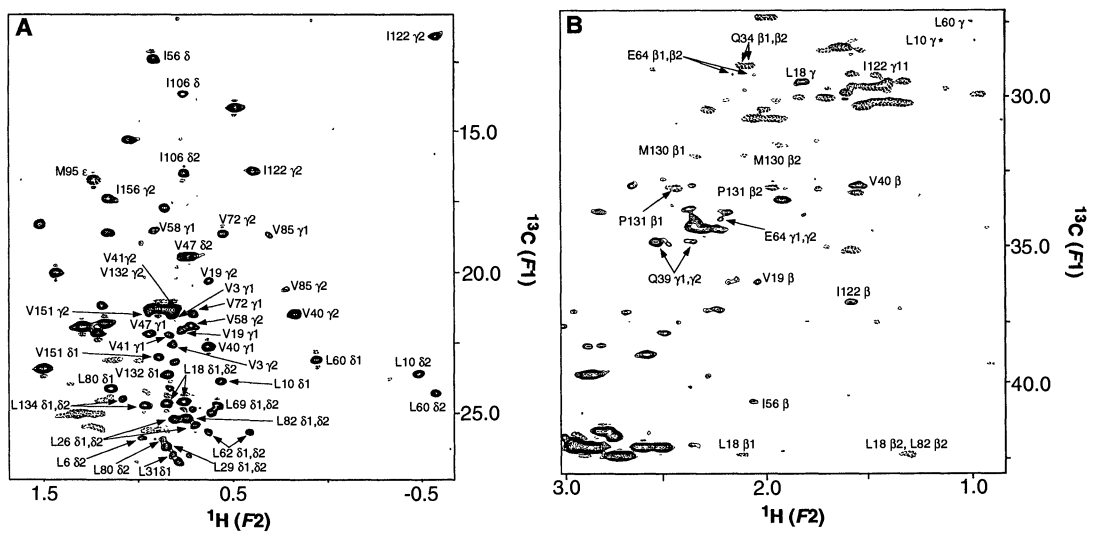

Fig. 1. Portions of the methyl (**A**) and methylene and methine (**B**) regions of the H_2O-NOE-^1H-^{13}C HSQC difference spectrum of ^{13}C-^{15}N–labeled hIL-β recording at 35°C with a mixing time of 60 ms. The signs of all the cross-peaks are the same as those in the sum reference spectrum, which indicates that the NOEs are all negative in sign. Note that the sign of the cross-peaks in the sum reference spectrum depends on the number of carbon atoms directly bonded to the carbon of interest, with carbon atoms bonded to even and odd numbers of carbon atoms giving rise to cross-peaks of opposite sign. Positive and negative cross-peaks are shown as continuous and dashed contour lines, respectively. Only cross-peaks involved in direct NOEs with water are labeled. For the remaining cross-peaks, an indirect mechanism involving an NOE with an exchangeable proton less than 5 Å away followed by chemical exchange with water cannot be excluded. The asterisk in (B) indicates the location of the cross-peak arising from the γ-methine group of Leu^{10}, which is below the contour level shown in the figure. Abbreviations for the amino acid residues are as follows: E, Glu; F, Phe; I, Ile; L, Leu; M, Met; P, Pro; Q, Gln; and V, Val.

intensities (attributable to the presence of three protons). In addition, however, we did see a number of NOEs and ROEs involving methylene protons. These included some NOEs to the β- and γ-methylene protons of a few Asp, Glu, and Gln residues at the surface of the protein(red spheres in Fig. 2). It should also be noted that, just as in the case of the GATA-1–DNA complex (*17*) and human thioredoxin (*18*), all surface-exposed methyl groups are hydrated. The fact that most of these are not associated with water in the crystal structures simply reflects the fact that the hydration water is positionally disordered. For example, this may be due to rapid independent rotation of a water pentagon around a rotating methyl group (*17*). This result lends credence to the concept of hydrophobic hydration (*19*).

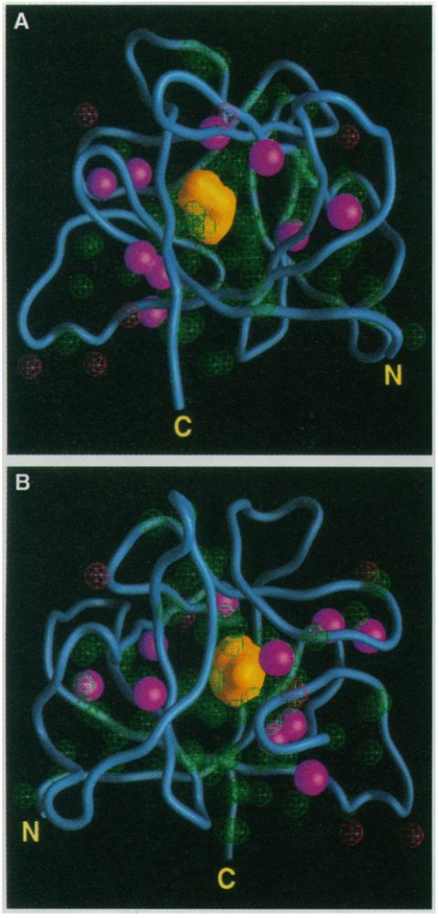

Fig. 2. Ribbon diagram of the solution structure of hIL-1β (blue) viewed from the front (**A**) and back (**B**) of the β barrel, showing the location of groups giving rise to NOEs with bound water, crystallographically conserved water molecules observed by NMR, and the central hydrophobic cavity. The protons giving rise to NOEs are abstracted to their directly bonded carbon atom and are displayed as green (hydrophobic residues) and red (polar residues) line spheres with a radius of 1.2 Å; the crystallographically conserved water molecules are depicted as solid magenta spheres with a radius of 1.6 Å; the surface of the hydrophobic cavity is shown in yellow. The volume and surface area of the cavity, calculated with a probe radius of 1.4 Å with the use of the program GRASP (*30*), are 125 Å^3 and 137 Å^2, respectively. [This procedure when applied to the coordinates of T4 lysozyme and its cavity-generating mutants yields values for the cavity volumes and surface areas that are very similar to those cited in (*8*).] The coordinates are taken from (*14*), and the location of the crystallographically conserved water molecules from (*13*). The figure was generated with the program GRASP (*30*). C, COOH-terminus; N, NH_2-terminus.

Examination of the hIL-1β structure revealed the presence of a large internal hydrophobic cavity that, on the basis of the NMR data, must be filled with water. It was located at the center of the molecule bounded by the six-stranded β barrel in the front (strands 1, 4, 5, 8, 9, and 12) and the remaining six strands at the rear (strands 2, 3, 6, 7, 10, and 11). The volume of the cavity varied from 75 to 95 Å^3 in the three crystal structures (*13*) to 125 Å^3 in the NMR structure (*14*). Thus, it can potentially accommodate two to four water molecules if one assumes that the density of water within the cavity is the same as that of the bulk solvent (*20*). The residues pointing toward the cavity were entirely hydrophobic, and there were no potential backbone hydrogen bond donors or acceptors that could interact with water. NOEs to water were observed from the methyl protons of Leu^{10}, Leu^{18}, Leu^{26}, Leu^{60}, Leu^{69}, Leu^{80}, Ile^{122}, and Val^{132}; from the β-methylene protons of Leu^{10} and Leu^{18}; from the γ-methine protons of Leu^{10}, Leu^{18}, and Leu^{60}; and from the β-methine and γ-methylene protons of Ile^{122} (Fig. 3). In addition to these residues, the aromatic rings of Phe^{42}, Phe^{112}, and Phe^{146} lined the cavity. There were no NOEs observed between these three aromatic residues and water. This was a result of the rapid relaxation of aromatic protons in concert with strong coupling of aromatic carbons, which results in a large decrease in sensitivity relative to that of the methyl groups.

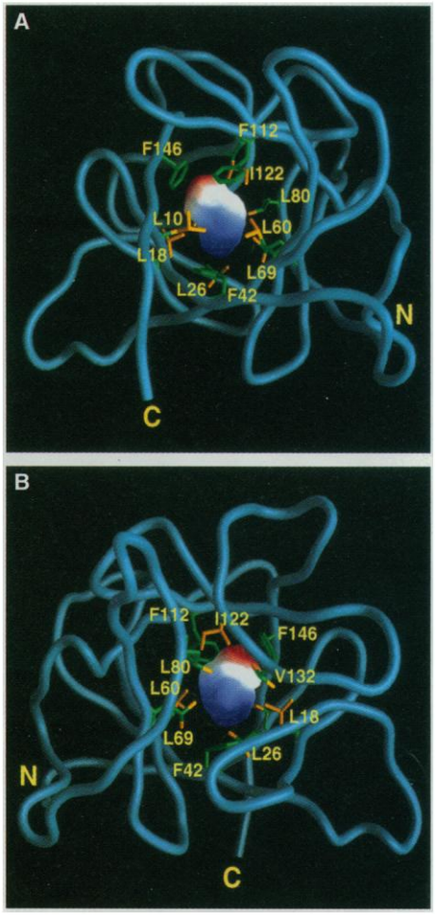

Fig. 3. Ribbon diagram of the solution structure of hIL-1β (blue) viewed from the front (**A**) and back (**B**) of the β barrel, showing the side chains involved in NOEs with hydration water in the central hydrophobic cavity. The carbon atoms directly bonded to the protons that gave rise to NOEs with water in the central cavity are depicted in orange; the remaining carbon atoms of the side chains are shown in green. The electrostatic potential in the cavity, calculated as described (*23*), is color-coded with red and blue representing negative and positive potentials, respectively. The coordinates are taken from (*14*); the figure was generated with the program GRASP (*30*). Abbreviations are as in Figs. 1 and 2.

The internal cavity appeared to be empty in all three crystal structures of hIL-1β. This cannot be attributed to low occupancy of water molecules within the cavity. Under such circumstances, the water would not be observable either by crystallography or by NMR. For example, an occupancy of 10% would reduce the NOE intensities by a factor of 10. Because the intensities of the observed NOEs to water within the cavity are among the highest observed and are of an intensity comparable to that involving structural waters that are detectable by crystallography at high occupancy (Fig. 1), a situation in which the cavity would be empty in a major (~90%) species, but filled in a minor (~10%) one (perhaps an open form that permitted rapid exchange with solvent) is unlikely. Consequently, the bound water within the hydrophobic cavity observed by NMR is in all likelihood positionally disordered and present at high occupancy (near unity). Such positional disorder, coupled with the presence of several water molecules within the cavity, would not attenuate the NOE cross-peaks (*4*, *5*) but would make them invisible crystallographically (*2*). It is perhaps worth noting that if only a single water molecule were present in the cavity, positional disorder would result in some attenuation of the cross-peaks owing to $\langle r^{-6}\rangle^{-1/6}$ averaging (where r is distance).

The central cavity can communicate to the exterior via two small channels. One is located at the opening of the β barrel (front of Fig. 3A) and has dimensions of 1.9 Å by 0.4 Å in cross section; the other is located at the back of the β barrel (front of Fig. 3B) and has dimensions of 1.7 Å by 1.6 Å in cross section. Although both channels are too narrow to permit the penetration of water molecules, one would expect them to open transiently during fluctuations that are known to occur, as evidenced by rapid aromatic ring flipping. As the NOEs are observed at the resonance of bulk water, one can conclude that the water molecules in the cavity are in fast exchange with solvent water on the time scale of the chemical shift. This, together with the observation of sizable negative NOEs (Fig. 1), indicates that these water molecules are long-lived, with a residency time ranging from a lower limit of 1 to 2 ns to an upper limit of 100 to 200 μs.

Can it be energetically favorable for water to occupy a cavity that is surrounded by nonpolar residues? Upon transferring a small molecule with a large dipole [$\mu \sim 0.4$ *e*Å for water (*21*)] from the solvent to the cavity, the most significant change in free energy probably arises from less favorable electrostatic interactions with the nonpolar environment. To estimate this increase in free energy for a water molecule, we modeled the water molecule as a spherical region (with radius a and dielectric constant ε_w) that carries a dipole μ at its center and is embedded in the surrounding medium (with dielectric constant ε_m). In such a model, the electrostatic interaction energy of the dipole with the surrounding medium is (*22*)

$$-332(\varepsilon_m - \varepsilon_w)\mu^2/(2\varepsilon_m + \varepsilon_w)\varepsilon_w a^3 \quad (1)$$

Taking ε_w to be 2 (*22*) and a to be 1.4 Å, this formula gives values of −4.7 and −2.0 kcal mol^{-1}, respectively, for the electrostatic interaction energy of the dipole of the water molecule with the bulk solvent (ε_m = 78.5) and with the nonpolar environment of the cavity [assuming ε_m = 4 for the protein (*23*)]. Thus, it costs about 2.7 kcal mol^{-1} to transfer a water molecule from the solvent to the cavity.

The water molecule, however, may be stabilized by favorable interactions with the charges of the protein. To see if such stabilization occurs, we calculated the electrostatic potential generated by the protein charges in the cavity. In this calculation, the protein is modeled as a low dielectric region embedded in a high dielectric solvent (*23, 24*) (Fig. 3). The electrostatic potential at the two ends of the cavity is opposite in sign and thus indeed stabilizes the dipole of a water molecule. The potential, however, would have been negative in the entire cavity if the high dielectric solvent had not been taken into consideration. Thus, the sign reversal at one end of the cavity arises from polarization charges on the dielectric boundary between the protein and the solvent. The electrostatic field E in many regions of the cavity is between 2 and 4 kcal mol^{-1} e^{-1} Å^{-1}. This lowers the free energy of a water molecule ($E\mu$) by 1 to 2 kcal mol^{-1} and offsets a substantial portion of the cost of transferring the molecule from the solvent to the cavity. (It should be noted that sign reversal of the electrostatic potential per se is not a requirement for stabilization of a dipole, as all that is needed is a gradient of the potential.)

Several other factors may further stabilize the water within the hydrophobic cavity. First, a water molecule may form weak hydrogen bonds with the aromatic rings (*25*) of Phe^{42}, Phe^{112}, and Phe^{146}, which line the cavity. Although these hydrogen bonds are electrostatic in nature, their contribution to the stabilization of water within the cavity may be underestimated in the electrostatic calculation presented above. Second, the interaction energy of a water molecule with the surrounding medium may be decomposed into electrostatic and nonelectrostatic components. Our calculation shows that the electrostatic component (arising from the dipole of the water molecule) may somewhat favor the solvent. The dominant portion of the nonelectrostatic component is the entropic contribution arising from the rearrangement of molecules around the solute (that is, the water molecule under consideration, which may be modeled as a spherical region without the dipole when dealing with nonelectrostatic effects). The difference in entropic contribution between the solvent and the nonpolar environment of the cavity is just the effect of hydrophobic interactions and can be estimated from the free energies of transferring nonpolar groups from water to organic solvents. When the surface area of a water molecule (~35 Å^2) is multiplied by the proportionality constant between transfer free energy and surface area [0.025 kcal mol^{-1} Å^{-2} (*26*)], we find that the nonelectrostatic component favors the cavity by ~0.9 kcal mol^{-1}. Third, if more than one water molecule occupies the cavity, hydrogen bonding between these molecules will be strengthened in the low dielectric cavity (*27*). This will compensate for any loss of entropy that is a result of the confinement within the cavity. Such loss of entropy should be small, as suggested by the fact that the cavity water is positionally disordered. Finally, occupation of a potential vacuum at the center of the protein increases the entropy of the protein-solvent system.

In the light of these arguments, it therefore seems likely that the presence of positionally disordered water within an internal, moderately sized hydrophobic cavity is energetically more favorable than its absence. In this regard, it is interesting to note that the central hydrophobic cavity is conserved in all other members of the β-trefoil class of proteins (*12*), for which complete coordinates have been deposited in the Brookhaven Protein Data Bank. These include mouse IL-1β, basic and acidic fibroblast growth factor, and the Kunitz inhibitor from *Erythrina cafra* (*28*). In the case of mouse IL-1β the size of the cavity is the same as that of hIL-1β, whereas for the other three proteins it is approximately half that size. This observation suggests that the central hydrophobic cavity is a common feature of the β-trefoil class of proteins, which arises as a result of the limited nature of the available amino acid side chains to fill the space generated by the fold. Just as in the crystal structures of hIL-1β, the cavity appears empty in the crystal structures of these four proteins, indicating that any water present is positionally disordered. As the stabilizing forces discussed above are not unique to hIL-1β, we suspect that the occurrence of positionally disordered water in large hydrophobic cavities is a common phenomenon and that some of the crystallographically empty hydrophobic cavities generated in a variety of mutants of T4 lysozyme (*8*) and ribonuclease A (*9*) may also be filled with positionally disordered water.

REFERENCES AND NOTES

1. J. T. Edsall and H. A. McKenzie, *Adv. Biophys.* **16**, 55 (1983); J. L. Finney, *Philos. Trans. R. Soc. London Ser. B* **278**, 3 (1977); E. Westhof, *Water and Biological Macromolecules* (CRC Press, Boca Raton, FL, 1993).
2. M. Levitt and B. H. Park, *Structure* **1**, 223 (1993).
3. G. A. Jeffery and W. A. Saenger, *Hydrogen Bonding in Biological Structures* (Springer-Verlag, Berlin, 1991); P. A. Karplus and C. Faerman, *Curr. Opin. Struct. Biol.* **14**, 770 (1994); J.-S. Jiang and A. T. Brünger, *J. Mol. Biol.* **243**, 100 (1994).
4. G. Otting and K. Wüthrich, *J. Am. Chem. Soc.* **111**, 1871 (1989); G. Otting, E. Liepinsh, K. Wüthrich, *Science* **254**, 974 (1991).
5. G. M. Clore, A. Bax, P. T. Wingfield, A. M. Gronenborn, *Biochemistry* **29**, 5671 (1990).
6. F. M. Richards, *Annu. Rev. Biophys. Bioeng.* **6**, 151 (1977).
7. A. A. Rashin, M. Iofin, B. Honig, *Biochemistry* **25**, 3619 (1986); M. A. Williams, J. M. Goodfellow, J. M. Thornton, *Protein Sci.* **3**, 1224 (1994); S. J. Hubbard, K.-H. Gross, P. Argos, *Protein Eng.* **7**, 613 (1994).
8. A. E. Eriksson *et al.*, *Science* **255**, 178 (1992).
9. R. Varadarajan and F. M. Richards, *Biochemistry* **31**, 12315 (1992).
10. A. A. Kossiakoff, M. D. Sintchak, J. Shpungin, L. G. Presta, *Proteins* **12**, 223 (1992).
11. R. Wolfenden and A. Radzicka, *Science* **265**, 936 (1994).
12. A. D. McLaghlan, *J. Mol. Biol.* **133**, 557 (1979); A. G. Murzin, A. M. Lesk, C. Chothia, *ibid.*. **223**, 531 (1992).
13. B. C. Finzel *et al.*, *ibid.* **209**, 779 (1989); J. P. Priestle, H. P. Schär, M. G. Grütter, *Proc. Natl. Acad. Sci. U.S.A.* **86**, 9667 (1989); B. Veerapandian *et al.*, *Proteins* **12**, 10 (1992).
14. G. M. Clore, P. T. Wingfield, A. M. Gronenborn, *Biochemistry* **30**, 2316 (1991).

15. All NMR experiments were carried out on a 1.7 mM sample of uniformly labeled (>95%) ^{13}C-^{15}N hIL-1β, at pH 5.4 in 150 mM sodium acetate-d_3 buffer dissolved in 90% H_2O–10% D_2O. The sample of hIL-1β was expressed, labeled, and purified as described (*13*). The spectra were recorded on a Bruker AMX600 spectrometer equipped with a triple resonance self-shielded *z* gradient probe. The 2D H_2O NOE-ROE-^1H-^{13}C HSQC experiments were carried out exactly as described in (*17*) with the use of the water flip-back technique to avoid saturating the water (*16*). The NOE spectra were recorded with mixing times of 60, 100, and 200 ms at 35°C and 60 ms at 20°C, whereas the ROE spectra were recorded at mixing times of 30 ms at both 20° and 35°C. In addition, a control H_2O-NOE-^1H-^{13}C HSQC spectrum with a mixing time of 100 ms was recorded with weak presaturation of the water resonance followed by a 200-ms delay before the first selective ^1H pulse (*17*) [S. Grzesiek *et al.*, *J. Am. Chem. Soc.* **116**, 1581 (1994)]. In this control spectrum, all interactions with water were attenuated (about 20-fold), whereas NOEs to protons attached to ^{12}C, which resonate in the vicinity of the water resonance, were essentially unaffected. All the cross-peaks observed in the H_2O-NOE^1-H-^{13}C HSQC difference spectra were suppressed in the control difference spectrum, which indicates that they arise solely from interactions with water (either direct or indirect by means of an exchangeable proton). By recording NOE spectra at several mixing times, as well as ROE spectra, we could ascertain that the cross-peaks attributable to NOEs with water were not the result of spin-diffusion. The spectra were processed with NmrPipe [F. Delaglio *et al.*, in *Proceedings of the 35th Experimental Nuclear Magnetic Resonance Conference* (Asilomar, CA, abstract WP108, 1994), p. 262] and were displayed and analyzed with the programs CAPP and PIPP [D. S. Garrett, R. Powers, A. M. Gronenborn, G. M. Clore, *J. Magn. Reson.* **95**, 214 (1991)]. The spectral assignments were taken from G. M. Clore, A. Bax, P. C. Driscoll, P. T. Wingfield, and A. M. Gronenborn [*Biochemistry* **29**, 8172 (1990)].
16. S. Grzesiek and A. Bax, *J. Biomol. NMR* **3**, 627 (1993); *J. Am. Chem. Soc.* **115**, 12593 (1993).
17. G. M. Clore, A. Bax, J. G. Omichinski, A. M. Gronenborn, *Structure* **2**, 89 (1994).
18. J. Qin, G. M. Clore, A. M. Gronenborn, *ibid.*, p. 503.
19. L. R. Pratt and D. Chandler, *J. Chem. Phys.* **73**, 3430 (1980); G. Ravishanker, M. Mezei, D. L. Beveridge, *Faraday Symp. Chem. Soc.* **17**, 70 (1982); G. I. Makhatadze and P. L. Privalov, *J. Mol. Biol.* **232**, 639 (1993); P. L. Privalov and G. I. Makhatadze, *ibid.*, p. 660; J. Walshaw and J. M. Goodfellow, *ibid.* **231**, 392 (1993).
20. Given that bulk water has a concentration of 55 M, the number of water molecules per cubic angstrom was calculated to be 0.033.
21. F. J. Lovas, *J. Phys. Chem. Ref. Data* **7**, 1445 (1978).
22. The dielectric boundary between the spherical region representing the water molecule and the surrounding medium induces a reaction field E_r at the center of the spherical region. Using boundary conditions of the electrostatic potential, one finds (*29*)

$$E_r = 2(\varepsilon_m - \varepsilon_w)\mu/(2\varepsilon_m + \varepsilon_w)\varepsilon_w a^3$$

where ε_w and ε_m are the dielectric constants of the water molecule and surrounding medium, respectively, and *a* is the radius of a water molecule. The electrostatic interaction energy of the dipole with the surrounding medium is

$$-E_r\mu/2 = -(\varepsilon_m - \varepsilon_w)\mu^2/(2\varepsilon_m + \varepsilon_w)\varepsilon_w a^3$$

(a factor of 332 should be inserted if μ is in units of eÅ, *a* in units of Å, and the energy in units of kcal mol^{-1}). The dielectric constant ε_w of the spherical region representing the water molecule is due to electronic polarization (*29*) and should be small. We thus chose $\varepsilon_w = 2$. The change in the interaction free energy of a water molecule with surrounding water molecules from the vapor phase to the liquid phase has been estimated from the vapor pressure and density of water and is found to be −6.3 kcal mol^{-1} at 25°C [A. Ben-Naim and Y. Marcus, *J. Chem. Phys.* **81**, 2016 (1984)]. This is very close to the value (−7.1 kcal mol^{-1}) predicted by our simple model for the change in electrostatic interaction energy. The model gives +2.4 and −4.7 kcal mol^{-1}, respectively, for the electrostatic interaction energy in the vapor phase ($\varepsilon_m = 1$) and in the liquid phase ($\varepsilon_m = 78.5$). A small (that is, <1 kcal mol^{-1}) nonelectrostatic component that disfavors the liquid phase would further improve the agreement between the model prediction and the estimate from experimental data.
23. H.-X. Zhou, *Biophys. J.* **65**, 955 (1993).
24. We obtained the electrostatic potential by solving discrete versions of the integral equations, describing the electrostatic potential and its normal derivative on the protein surface as previously done (*23*). Human IL-1β has an overall charge of −*e*.
25. M. F. Perutz, G. Fermi, D. Abraham, C. Poyart, E. Bursaux, *J. Am. Chem. Soc.* **108**, 1064 (1986); M. Levitt and M. F. Perutz, *J. Mol. Biol.* **201**, 751 (1988).
26. C. Chothia, *Nature* **248**, 338 (1974).
27. A. Ben-Naim, *Solvation Thermodynamics* (Plenum, New York, 1987).
28. D. H. Ohlendorf, A. C. Terharne, P. C. Weber, J. J. Wendoloski, F. R. Salemme, Brookhaven Protein Data Bank, accession code 8I1B (1991); X. Zhu *et al.*, *Science* **251**, 90 (1991); Z. Zhang, L. S. Cousens, P. J. Barr, S. R. Sprang, *Proc. Natl. Acad. Sci. U.S.A.* **88**, 3446 (1991); S. Onesti, P. Brick, D. M. Blow, *J. Mol. Biol.* **217**, 153 (1991).
29. T.-W. Lee and R. Zwanzig, *J. Chem. Phys.* **52**, 6353 (1970).
30. A. J. Nicholls, K. Sharp, B. Honig, *Proteins* **11**, 281 (1991).
31. We thank D. Garrett and F. Delaglio for software development; R. Tschudin for developing and building the pulsed field gradient accessory; and A. Bax, K. Frank, S. Grzesiek, A. Karplus, J. Kuszewski, P. Lodi, J. Qin, A. Szabo, and A. Wang for numerous helpful discussions. R.T.C. acknowledges a Leukemia Society of America postdoctoral fellowship. Supported by the AIDS Targeted Anti-Viral Program of the Office of the Director of the National Institutes of Health (G.M.C. and A.M.G.).

7 October 1994; accepted 12 January 1995

DNA Topoisomerase and Recombinase Activities in Nae I Restriction Endonuclease

Kiwon Jo and Michael D. Topal*

Nae I endonuclease must bind to two DNA sequences for cleavage. Examination of the amino acid sequence of Nae I uncovered similarity to the active site of human DNA ligase I, except for leucine 43 in Nae I instead of the lysine essential for ligase activity. Changing leucine 43 to lysine 43 (L43K) changed Nae I activity: Nae I–L43K relaxed supercoiled DNA to yield DNA topoisomers and recombined DNA to give dimeric molecules. Interruption of the reactions of Nae I and Nae I–L43K with DNA demonstrated transient protein-DNA covalent complexes. These findings imply coupled endonuclease and ligase domains and link Nae I endonuclease to the topoisomerase and recombinase protein families.

Topoisomerases, recombinases, and endonucleases share the ability to cleave DNA but do not have sequence homology. Topoisomerases catalyze DNA relaxation by cleavage, strand passage, and reunion; recombinases catalyze DNA rearrangements by concerted cleavage and exchange of DNA ends; and endonucleases catalyze cleavage of single- and double-stranded DNA. These enzymes are ubiquitous and essential for replication, transcription, recombination, and repair of DNA (*1*). Although there has been speculation on their evolution, no relation among these enzymes has been found. Endonucleases include as a special class the restriction enzymes, which in bacteria protect against foreign DNA. The restriction enzymes, along with the site-specific recombinases, offer examples of sequence-specific DNA cleavage. Topoisomerases generally demonstrate sequence preferences but are not sequence-specific.

The placing of restriction enzymes in a separate category from the topoisomerases and recombinases has been called into question by recent discoveries with the type IIe restriction enzymes. It is now clear that the type IIe enzymes require the recognition of a second DNA (effector) sequence to cleave DNA; moreover, there is homology between the type IIe enzyme Eco RII and the integrase family of proteins (*2*). These findings indicate complexities in the type IIe enzymes beyond that needed for restriction. The type IIe enzymes include Nae I (*3*), Nar I, Bsp MI, Hpa II, Sac II (*4*), Eco RII (*5*), Atu BI, Cfr 9I, Sau BMKI, Eco 57I, and Ksp 632I (*6*), which represent a wide variety of bacterial species.

Nae I is a prototypical type IIe enzyme, a 70-kD dimeric protein (*7*) with two DNA binding sites, as indicated by its sigmoidal dependence of cleavage velocity on the concentration of recognition sequence (*8*). The two DNA binding sites of Nae I are nonidentical: one site prefers to bind to GCCGGC with AT-rich flanking sequences, whereas the other prefers to bind to GCCGGC with GC-rich flanking sequences (*8*). Whether the binding differences preexist or are induced upon occupation of one DNA binding site is unclear. Because Nae I must bind two DNA recognition sequences, a DNA substrate with a single Nae I recognition sequence can resist cleavage (*3*). This resistance can be overcome by the introduction of another DNA recogni-

Lineberger Comprehensive Cancer Center, Department of Biochemistry and Biophysics, and Department of Pathology, University of North Carolina Medical School, Chapel Hill, NC 27599, USA.

*To whom correspondence should be addressed.